Non-linear MHD code JOREK: Application and Development

Matthias Hölzl

JOREK

- Non-linear MHD code
- Divertor tokamaks including X-point(s)
- Focus on plasma edge simulations
- Originally developed at CEA Cadarache Huysmans and Czarny (2007)
- Reduced MHD in toroidal geometry (next slide)
- Other models:
  - Two-fluid extensions (M. Becoulet, S. Pamela)
  - Neutrals (C. Reux)
  - Full MHD
- Fortran 90/95
- MPI + OpenMP hybrid parallelization

Reduced MHD Equations

$$\frac{\partial \Psi}{\partial t} = \eta j - R\,[u, \Psi] - F_0 \frac{\partial u}{\partial \phi}$$

$$\frac{\partial \rho}{\partial t} = -\nabla \cdot (\rho \mathbf{v}) + \nabla \cdot (D_\perp \nabla_\perp\, \rho) + S_\rho$$

$$\frac{\partial (\rho T)}{\partial t} = -\mathbf{v} \cdot \nabla (\rho T) - \gamma \rho T \nabla \cdot \mathbf{v} + \nabla \cdot \left(K_\perp \nabla_\perp\, T + K_{||} \nabla_{||} T \right) + S_T$$

$$\mathbf{e}_\phi \cdot \nabla \times \left\{ \rho \frac{\partial \mathbf{v}}{\partial t} = -\rho (\mathbf{v} \cdot \nabla) \mathbf{v} - \nabla p + \mathbf{j} \times \mathbf{B} + \mu \Delta \mathbf{v} \right\}$$

$$\mathbf{B} \cdot \left\{ \rho \frac{\partial \mathbf{v}}{\partial t} = -\rho (\mathbf{v} \cdot \nabla) \mathbf{v} - \nabla p + \mathbf{j} \times \mathbf{B} + \mu \Delta \mathbf{v} \right\}$$

$$j \equiv -j_\phi = \Delta^* \Psi$$

$$\omega \equiv -\omega_\phi = \nabla^2_{pol}\, u$$

Variables: Ψ, u, j, ω, ρ, T, $\nu_{||}$

Ideal wall + Bohm boundary conditions

Definitions: $\mathbf{B} = \frac{F_0}{R} \mathbf{e}_\phi + \frac{1}{R} \nabla \Psi \times \mathbf{e}_\phi$ and $\mathbf{v} = -R \nabla u \times \mathbf{e}_\phi + \nu_{||} \mathbf{B}$

1. Numerical Aspects
2. ELM Simulations
3. Resistive Wall Model

Spatial Discretization

- Toroidal Fourier-decomposition
- 2D Bezier finite elements (isoparametric, C^0 and C^1)

  Czarny and Huysmans (2008)
- Remaining problems:
  - Fourier basis-functions non-local (N^2 matrix entries)
  - Problems at axis and X-point (not C^1)
  - Positivity not guaranteed

Time evolution: Fully implicit

- Time-Discretization ($\mathbf{u}^{n+1} = \mathbf{u}^n + \delta\mathbf{u}^n$):

  $$\dot{\mathbf{A}}(\mathbf{u}(t)) = \mathbf{B}(\mathbf{u}(t))$$

  $$\left[(1+\xi)\left(\frac{\partial \mathbf{A}}{\partial \mathbf{u}}\right)^n - \Delta t\theta\left(\frac{\partial \mathbf{B}}{\partial \mathbf{u}}\right)^n\right]\delta\mathbf{u}^n = \Delta t\ \mathbf{B}^n + \xi\left(\frac{\partial \mathbf{A}}{\partial \mathbf{u}}\right)^{n-1}\delta\mathbf{u}^{n-1}$$

- Crank-Nicholson: ($\theta = 0.5$, $\xi = 0$) or Gears: ($\theta = 1$, $\xi = 0.5$)
- Involves a linearization (Newton iteration stopped after one step)

$\Rightarrow$ Large sparse system of equations solved iteratively with GMRES

Time evolution

Pro Implicitness:
Time step not restricted by CFL condition

Con Convergence:
Preconditioner inefficient with strong non-linearities

Con Efficiency:
Limited scalability and large memory consumption
due to direct solver (in preconditioner)

What to do?

Linearization $\rightarrow$ Newton-iterations?

GMRES $\rightarrow$ Jacobian-free?

Preconditioner $\rightarrow$ Matrix-free method?

$\rightarrow$ New Postdoc **Emmanuel Franck** in Eric Sonnendrückers department

1. Numerical Aspects

2. ELM Simulations

3. Resistive Wall Model

Overview

Simulations performed

- Edge Localized Modes (ELMs) in typical AUG H-mode equilibrium
- Focus on early phase until non-linear saturation starts

Poloidal Flux Perturbation

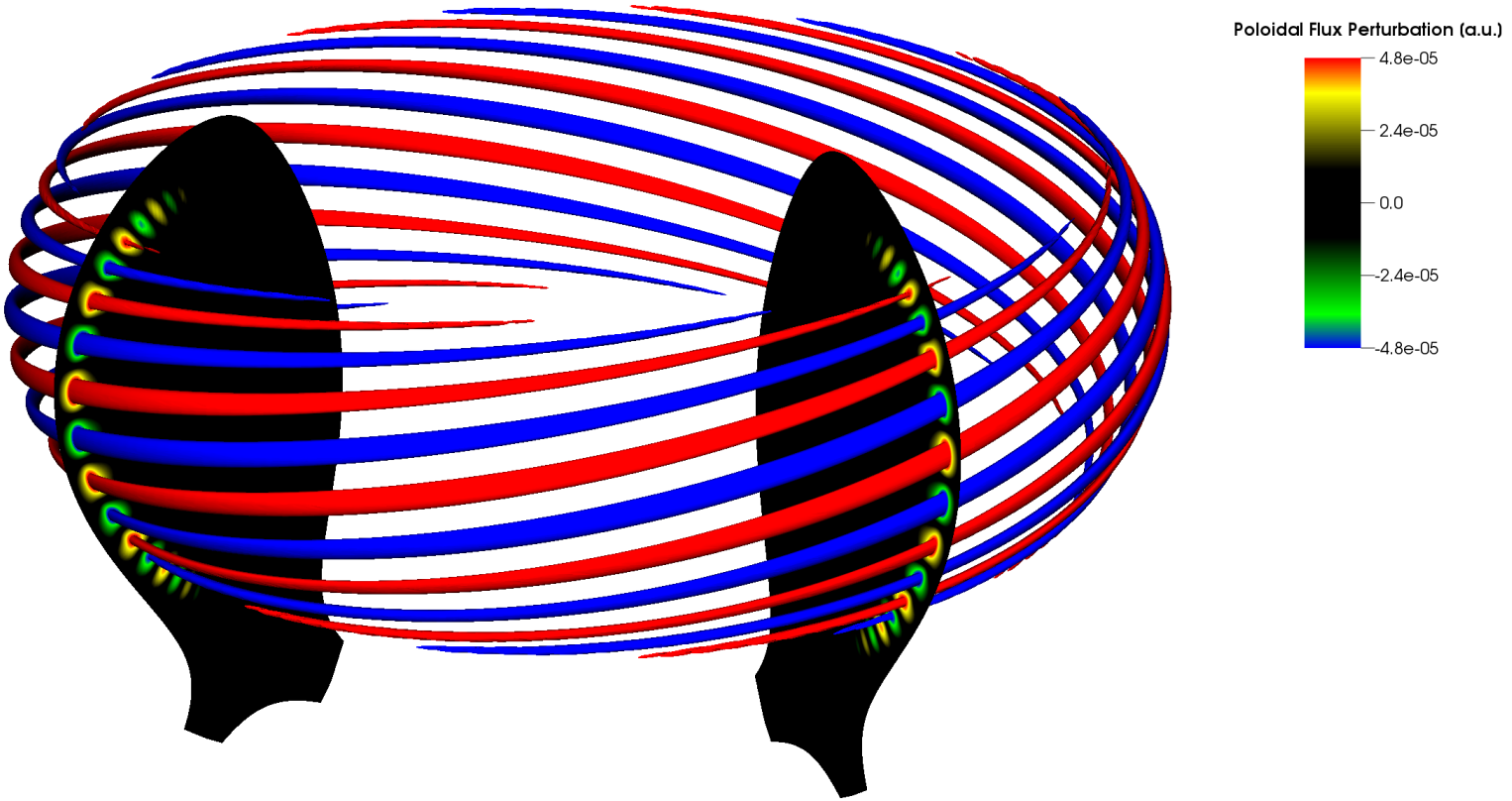

$n = 0, 8, 16$

- Red/blue surfaces correspond to 70 percent of maximum/minimum values

Poloidal Flux Perturbation

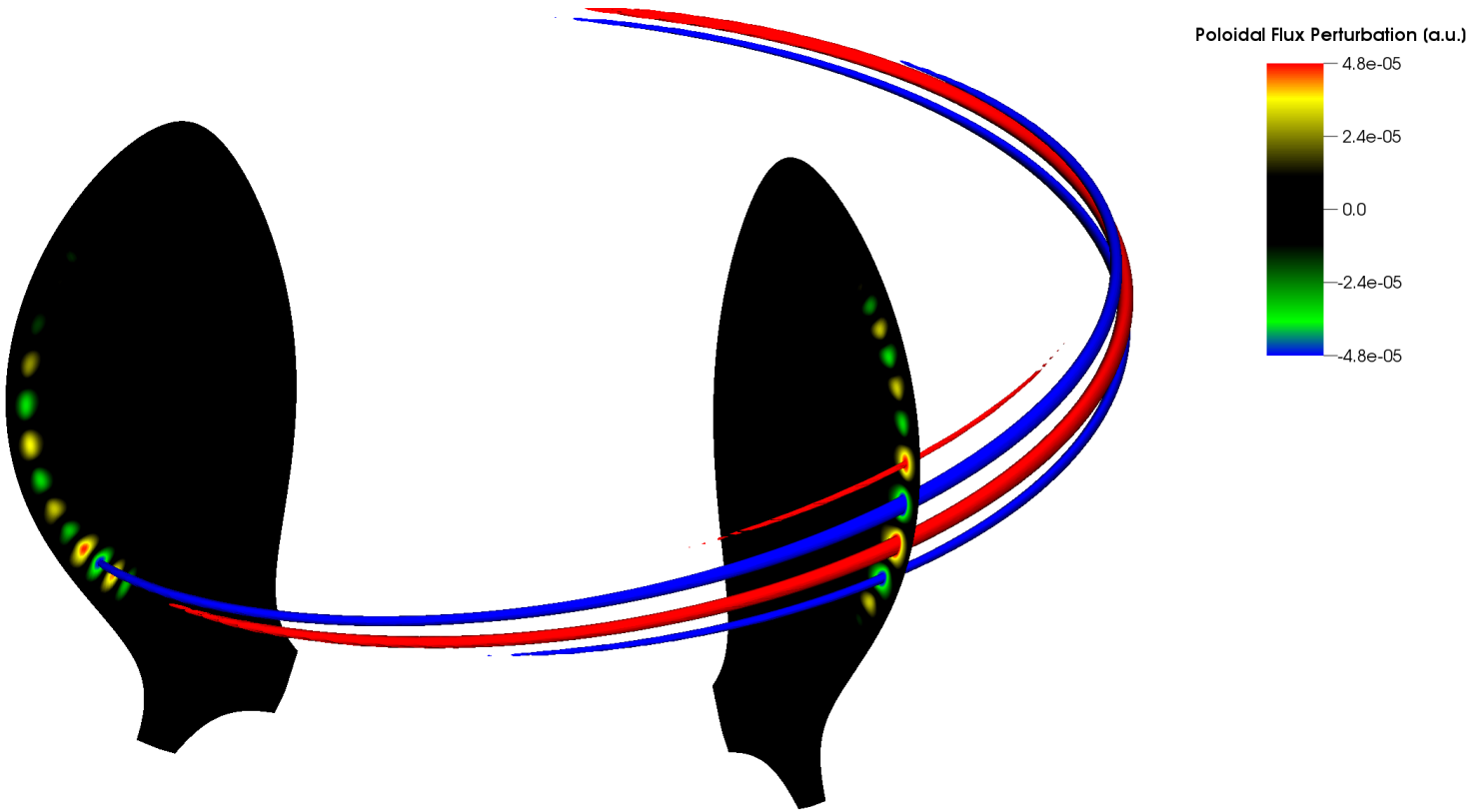

$$n = 0, 1, 2, 3, 4, \ldots, 16$$

- Red/blue surfaces correspond to 70 percent of maximum/minimum values
- Localized due to several strong modes with adjacent n
- $\sim$ Solitary Magnetic Perturbations in ASDEX Upgrade Wenninger et al. (2012)

Energy Timetraces

- $n = 1$ (and others) driven non-linearly to large amplitude (Subdominant modes not shown for clarity)

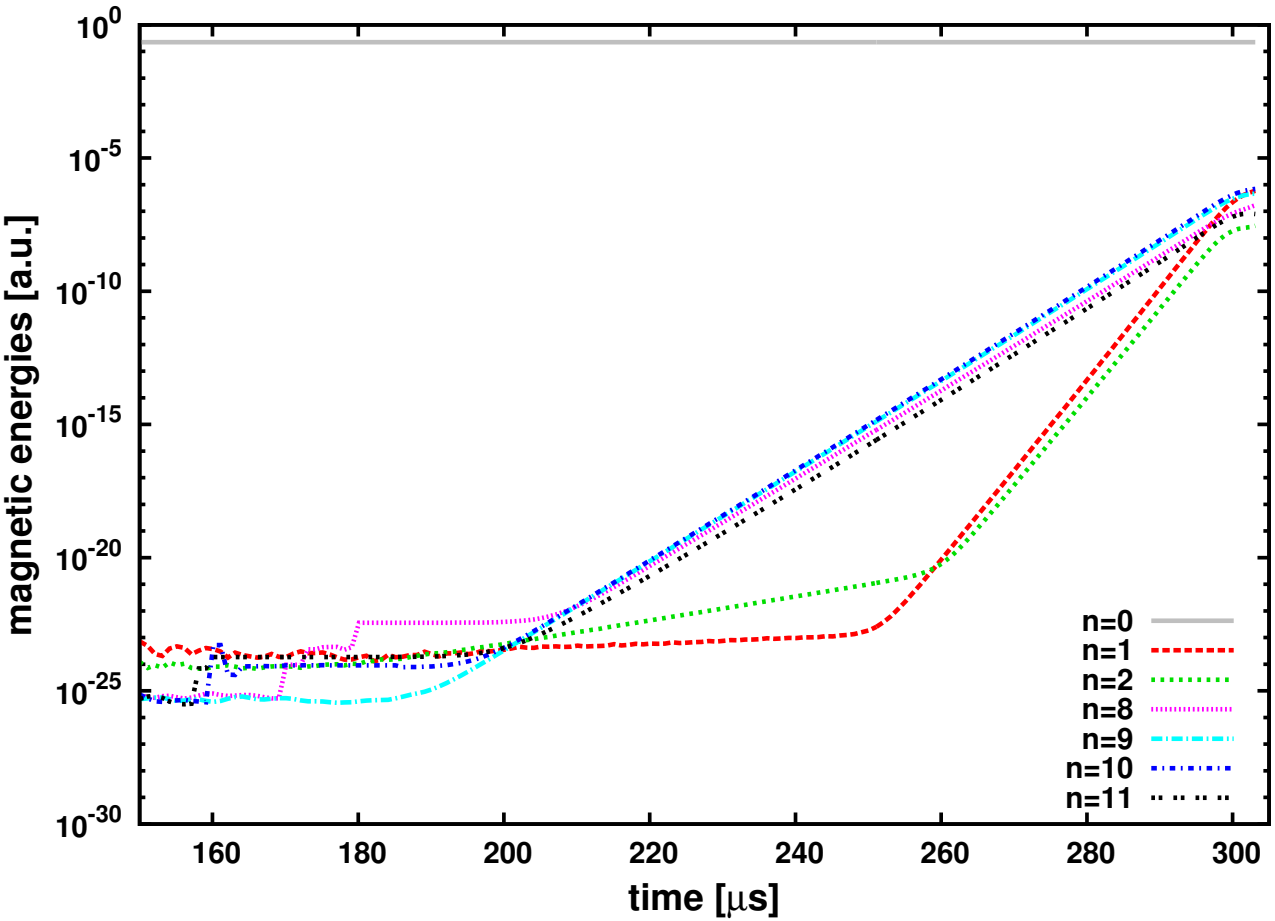

Mode Interaction

- Consider a case with $n = 0, 4, 8, 12, 16$ for the start
- Can we reproduce and understand this with a simple model?

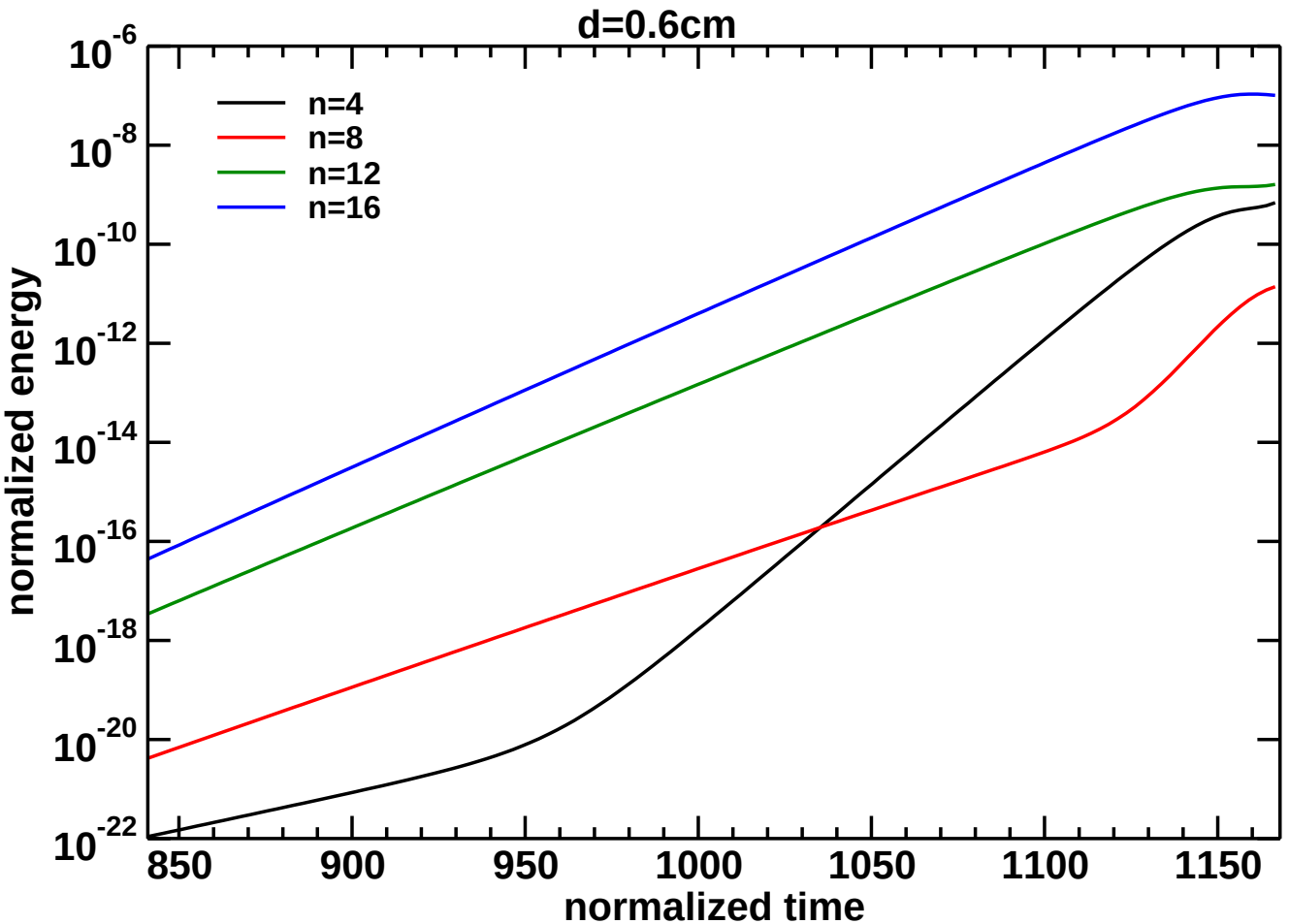

Mode Interaction (2)

- Non-linear terms lead to mixing of toroidal modes
- Quadratic: $(n_1, n_2) \leftrightarrow n_1 \pm n_2$
- For instance: $(8, 4)$, $(12, 8)$, and $(16, 12)$ couple to $n = 4$

Mode Interaction (2)

- Non-linear terms lead to mixing of toroidal modes
- Quadratic: $(n_1, n_2) \leftrightarrow n_1 \pm n_2$
- For instance: $(8, 4)$, $(12, 8)$, and $(16, 12)$ couple to $n = 4$
- Simple model (Mode rigidity, $n = 0$ fixed):

$$\dot{A}_4 = \overbrace{\gamma_4 \, A_4}^{\text{linear}} + \overbrace{\gamma_{8,-4} \, A_8 \, A_4 + \gamma_{12,-8} \, A_{12} \, A_8 + \gamma_{16,-12} \, A_{16} \, A_{12}}^{\text{non-linear interaction}}$$

Mode Interaction (2)

- Non-linear terms lead to mixing of toroidal modes
- Quadratic: $(n_1, n_2) \leftrightarrow n_1 \pm n_2$
- For instance: $(8, 4)$, $(12, 8)$, and $(16, 12)$ couple to $n = 4$
- Simple model (Mode rigidity, $n = 0$ fixed):

$$\dot{A}_4 = \overbrace{\gamma_4 \, A_4}^{\text{linear}} + \overbrace{\gamma_{8,-4} \, A_8 \, A_4 + \gamma_{12,-8} \, A_{12} \, A_8 + \gamma_{16,-12} \, A_{16} \, A_{12}}^{\text{non-linear interaction}}$$

$$\dot{A}_8 = \gamma_8 \, A_8 + \gamma_{4,4} A_4 \, A_4 + \gamma_{12,-4} A_{12} \, A_4 + \gamma_{16,-8} \, A_{16} \, A_8$$

$$\dot{A}_{12} = \gamma_{12} \, A_{12} + \gamma_{4,8} \, A_4 \, A_8 + \gamma_{16,-4} \, A_{16} \, A_4$$

$$\dot{A}_{16} = \gamma_{16} \, A_{16} + \gamma_{8,8} \, A_8 \, A_8 + \gamma_{4,12} \, A_4 \, A_{12}$$

- Linear growth rates taken from JOREK simulation
- Energy conservation $\Rightarrow$ Six remaining free parameters $\gamma_{i,j}$
- Determine free parameters numerically by minimizing quadratic difference

Mode Interaction (3)

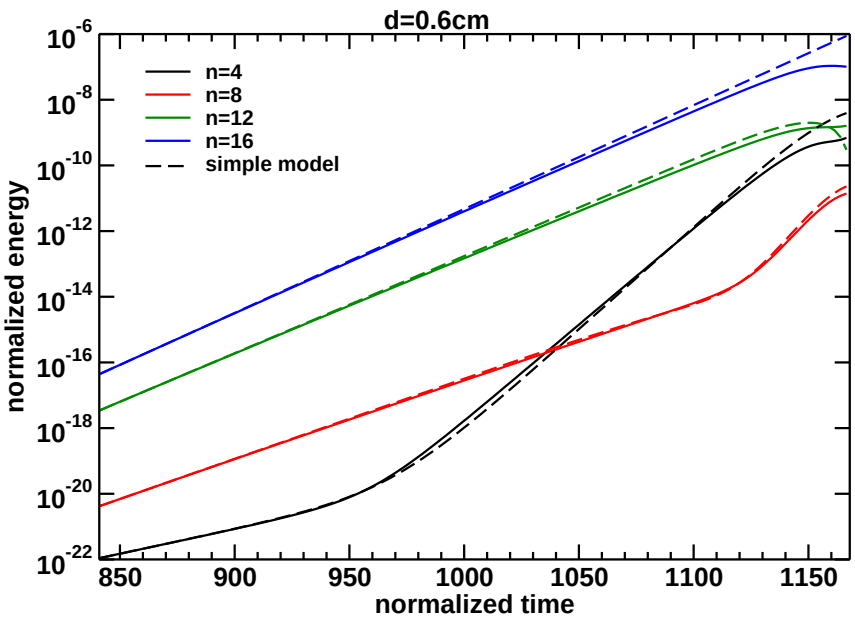

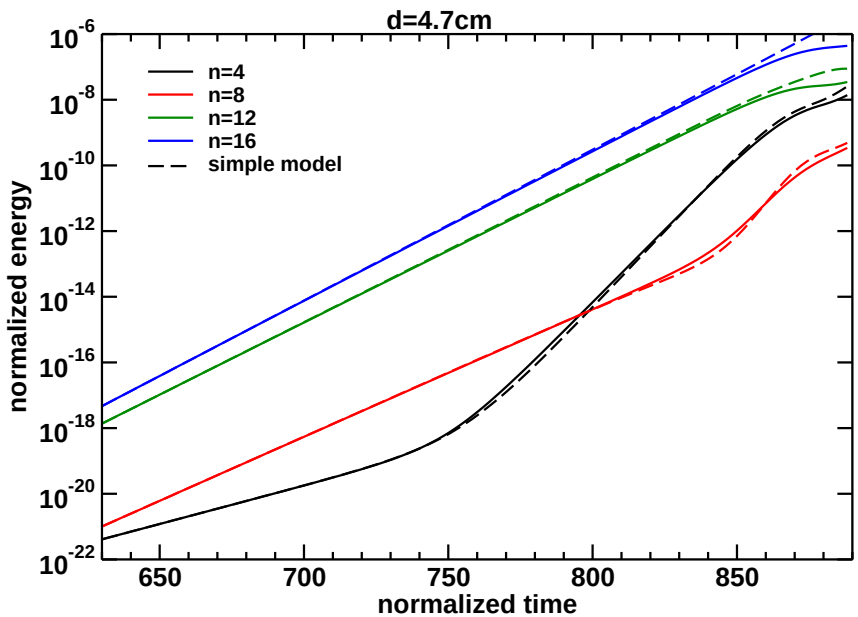

- Saturation not covered by the model (of course)
- Same set of interaction-parameters $\gamma_{i,j}$ for both wall-distances
- Non-linear growth described well
- Same mechanism brings up $n = 1$ in the simulations shown before with poloidally and toroidally localized ELMs!

Saturation

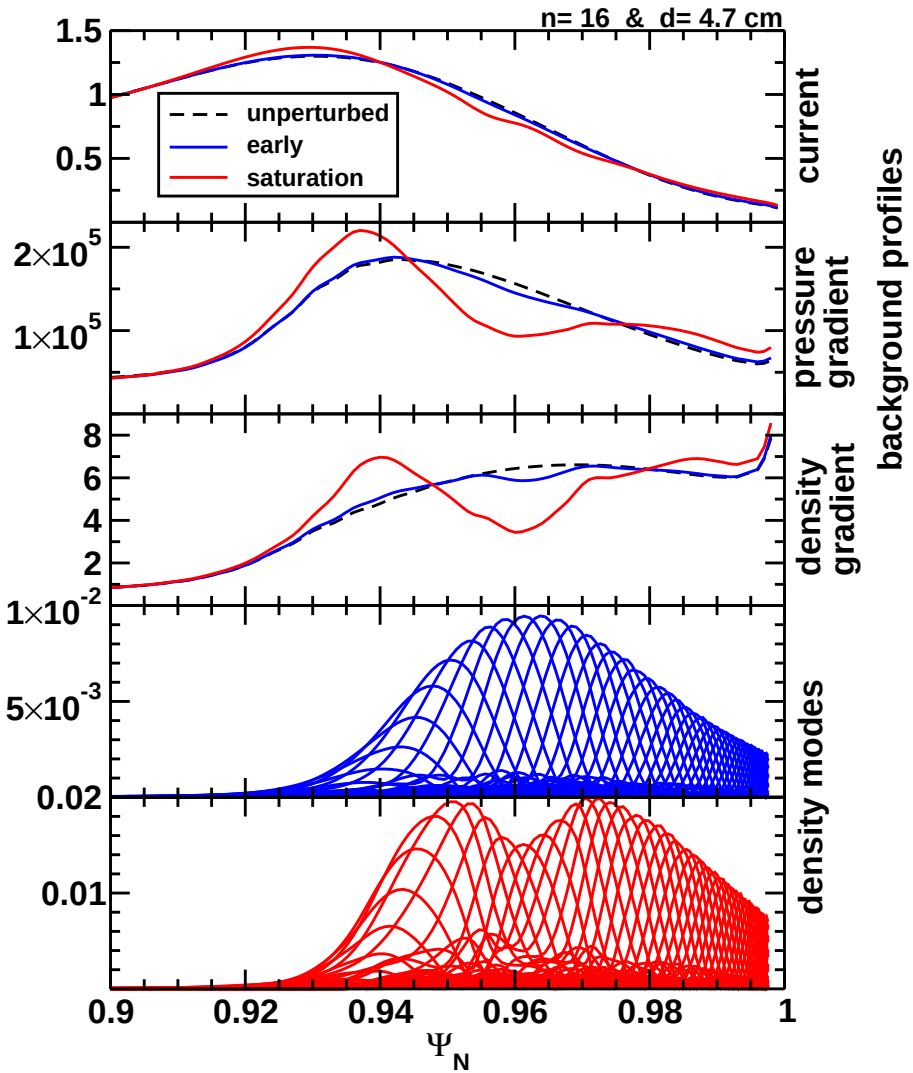

Saturation mechanisms:

- Displacement ξ gets significant compared to wall distance
- Modification of background profiles by the instability

Summary for this Part

- ELM simulations for realistic ASDEX Upgrade conditions
- Poloidal and toroidal localization of ELM-crash – similar to experiment
- $n = 1$ grows non-linearly – similar to experiment
- Can be explained by non-linear mode-interaction picture
- Saturation mechanisms
- Published in Hölzl et al. (2012a) and to be published in Krebs et al. (2013)

1. Numerical Aspects

2. ELM Simulations

3. Resistive Wall Model

Overview

Physics: Growing or rotating instabilities interact with conducting structures via eddy currents

For instance: External kink ($\sim \mu s$)

- With close-fitting ideal wall: Fully stabilized
- With resistive wall: Becomes a Resistive wall mode ($\sim ms$)
- May be fully stabilized by active feedback-system

Aim: Non-linear resistive wall simulations

Coupling of JOREK and STARWALL codes

Showing status of implementation and benchmarking

STARWALL

- Developed by Peter Merkel (Merkel and Sempf (2006); Strumberger et al. (2011))
- Version specifically written for JOREK
- Executed once for a JOREK simulation
- Conducting structures represented by triangles
  (3D structures including holes possible)
- Wall currents described by current potentials Y_k at triangle nodes
- Vacuum field equation solved outside JOREK domain
  (for set of unit Ψ-perturbations corresponding to Bezier DOFs)
- Gives **non-local expression for $\mathbf{B}_{\mathbf{tan}}$ in terms of Ψ** at the interface
  (response matrices)

Natural boundary condition

- Current definition equation $j = \Delta^* \Psi$ in weak form (test function v^*):

$$\int dV \, \frac{v^*}{R^2} \, j - \int dV \, v^* \, \nabla \cdot \left(\frac{1}{R^2} \nabla \Psi \right) = 0$$

- Partial integration:

$$\int dV \, \frac{v^*}{R^2} \, j + \int dV \, \frac{1}{R^2} \, \nabla v^* \cdot \nabla \Psi - \oint dA \, \frac{v^*}{R} \, \underbrace{(\nabla \Psi \cdot \hat{\mathbf{n}}/R)}_{\equiv B_{\mathtt{tan}}} = 0.$$

- Ideal-wall boundary conditions: Boundary integral vanishes in “old” JOREK
- Natural boundary condition: Replace $B_{\mathtt{tan}}$ by STARWALL response

Vacuum Response

- Ideal wall (algebraic expression):

$$B_{tan} = \sum_i b_i \sum_j \hat{M}^{id}_{i,j} \Psi_j$$

- Vacuum response: $\hat{M}^{id}$

Vacuum Response

- Ideal wall (algebraic expression):

$$B_{tan} = \sum_i b_i \sum_j \hat{M}^{id}_{i,j} \Psi_j$$

- Resistive wall:

$$B_{tan} = \sum_i b_i \left(\sum_j \hat{M}^{ee}_{i,j} \Psi_j + \sum_k \hat{M}^{ey}_{i,k} \Upsilon_k \right)$$

$$\dot{\Upsilon}_k = -\frac{\eta_w}{d_w} \hat{M}^{yy}_{k,k} \Upsilon_k - \sum_j \hat{M}^{ye}_{k,j} \dot{\Psi}_j$$

- Vacuum response: $\hat{M}^{id}$, $\hat{M}^{ee}$, $\hat{M}^{ey}$, $\hat{M}^{ye}$, $\hat{M}^{yy}$

Vacuum Response

- Ideal wall (algebraic expression):

$$B_{tan} = \sum_i b_i \sum_j \hat{M}^{id}_{i,j} \Psi_j$$

- Resistive wall:

$$B_{tan} = \sum_i b_i \left(\sum_j \hat{M}^{ee}_{i,j} \Psi_j + \sum_k \hat{M}^{ey}_{i,k} Y_k \right)$$

$$\dot{Y}_k = -\frac{\eta_w}{d_w} \hat{M}^{yy}_{k,k} Y_k - \sum_j \hat{M}^{ye}_{k,j} \dot{\Psi}_j$$

- Vacuum response: $\hat{M}^{id}$, $\hat{M}^{ee}$, $\hat{M}^{ey}$, $\hat{M}^{ye}$, $\hat{M}^{yy}$
- Discretize consistent with fully-implicit time evolution scheme
- Plug B_{tan} into boundary integral $\oint dA \; \frac{j_i^*}{R} \underbrace{(\nabla\Psi \cdot \hat{\mathbf{n}}/R)}_{\equiv B_{tan}}$

Freeboundary Equilibrium

- Same boundary-integral in Grad-Shafranov equation
- Allows to test parts (no time-evolution, no wall-currents)
- ITER-like limiter case as first test

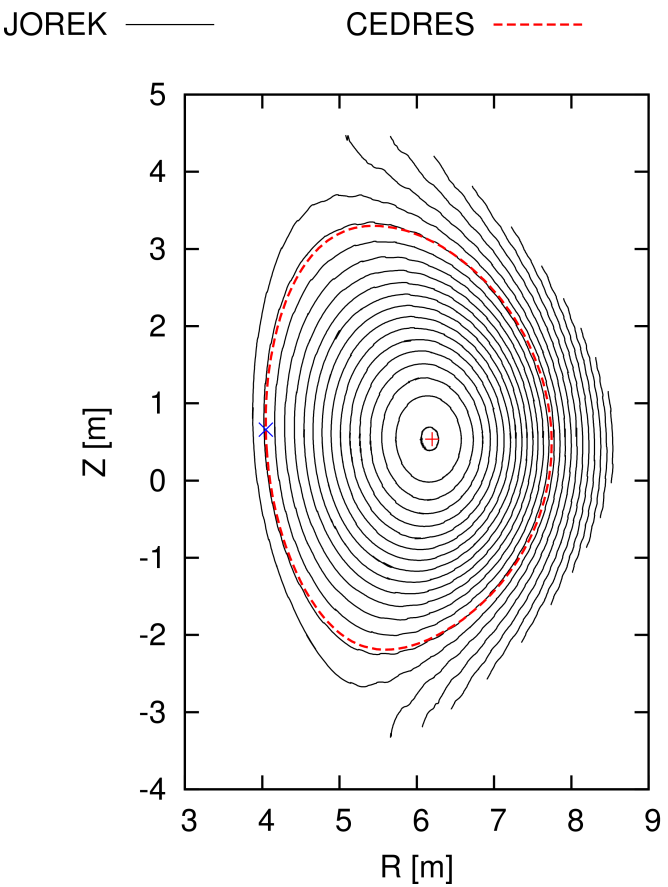

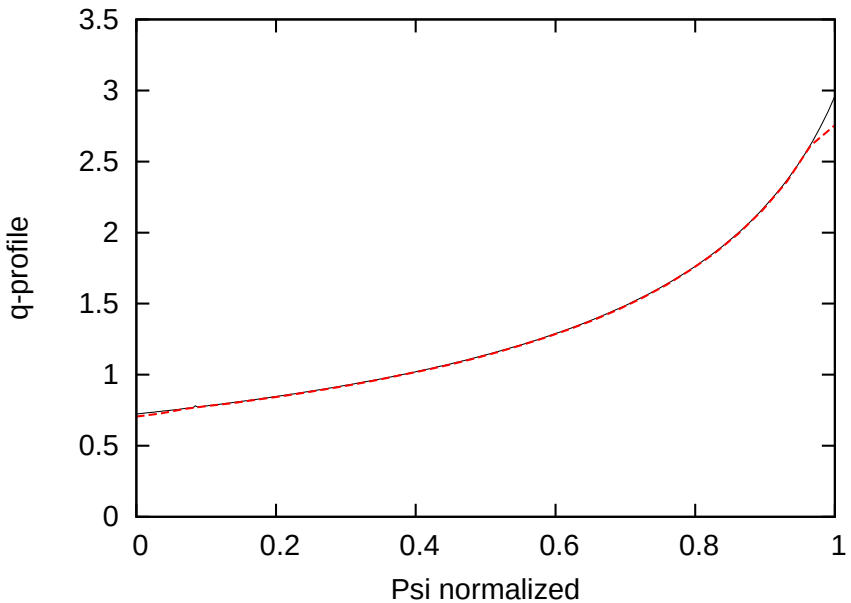

- Flux-surfaces and q-profile agree very well with CEDRES++

Tearing Mode

- 2/1 tearing mode in circular plasma ($R = 10$, $a = 1$)
- Concentric ideally conducting wall
- Linear growth rates:

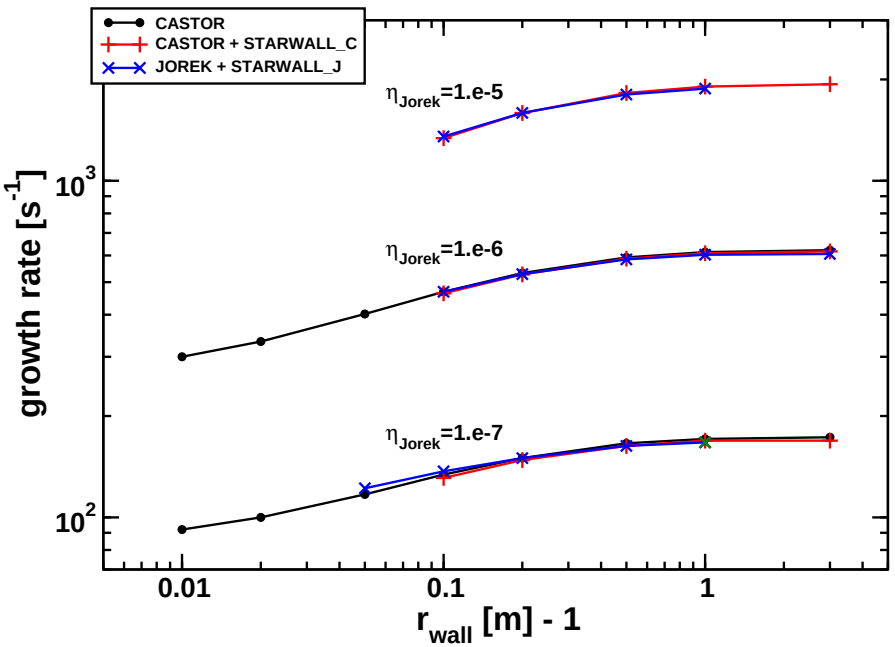

- Excellent agreement with linear CASTOR

External Kink Mode

- 2/1 external kink mode in circular plasma ($R = 10$, $a = 1$)
- Concentric resistive wall
- To be compared to analytical theory and linear simulations...

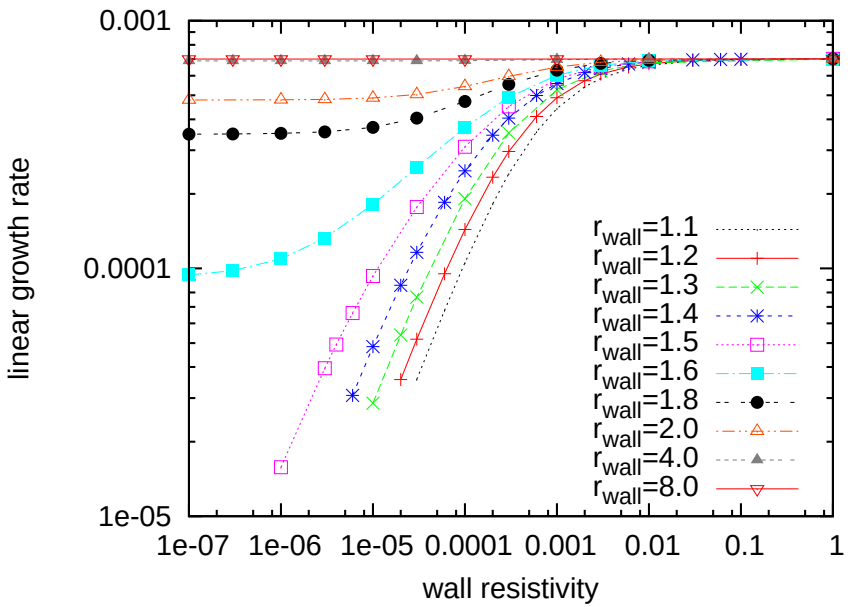

Linear growth rates for different wall radii and wall resistivities

External Kink Mode

- 2/1 external kink mode in circular plasma ($R = 10$, $a = 1$)
- Concentric resistive wall
- To be compared to analytical theory and linear simulations...

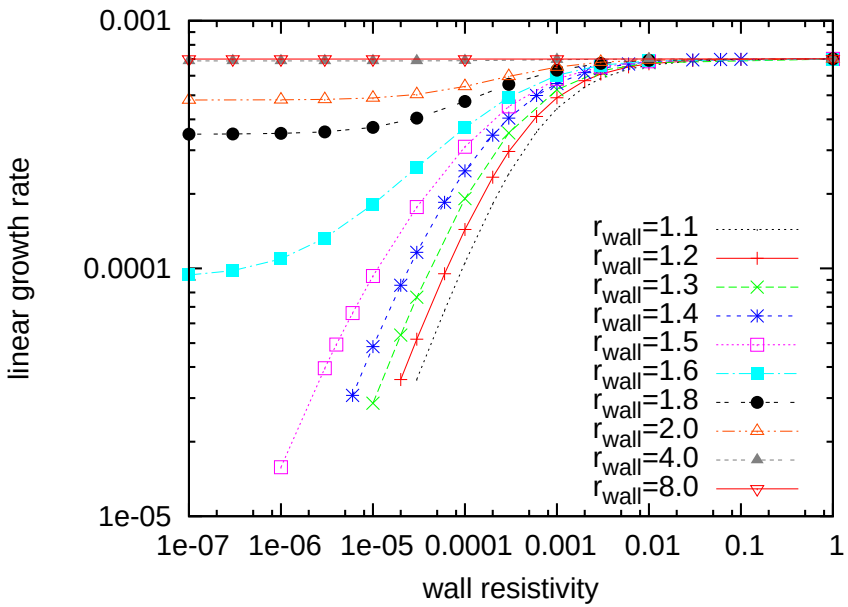

Linear growth rates for different wall radii and wall resistivities

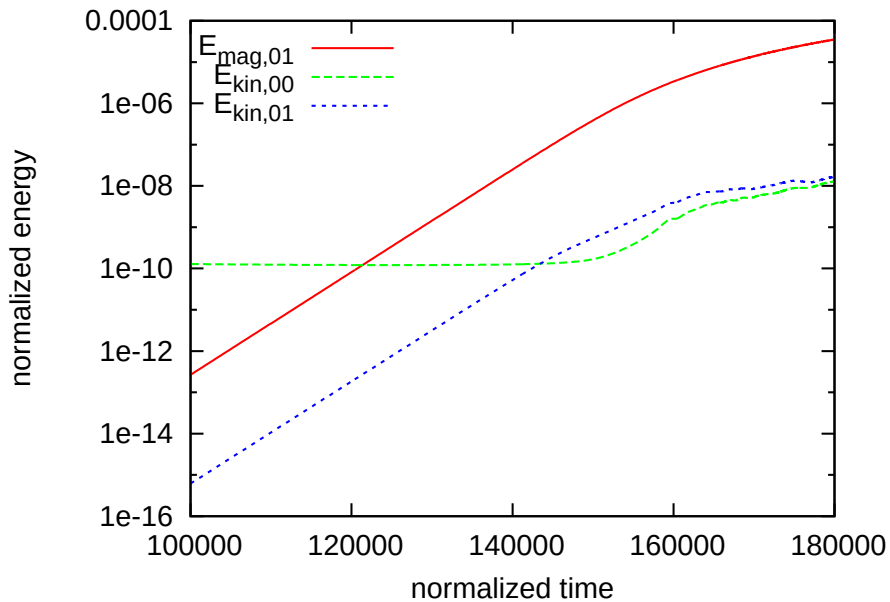

Example for non-linear saturation (stable, small time-steps for convergence)

Summary for this Part

- Plasma instabilities interact with conducting structures via eddy currents
- Aim: Non-linear investigations via coupling of JOREK and STARWALL
- Full-implicitness of JOREK time-integration is kept
- First tests with simplified geometry look promising
- Described in Hölzl et al. (2012b)

Summary and Outlook

Numerics

- Fully implicit, Bezier elements

→ New Postdoc working on this

ELM simulations for ASDEX Upgrade

- Poloidal and toroidal localization
- Low-n grow non-linearly

→ ELM-types? Affected region? Heat-flux patterns?

Resistive-wall model

- Implemented via coupling to STARWALL (some details remain to be done)
- Benchmarks ongoing

→ Non-linear simulations of RWMs, VDEs, . . .

References

O. Czarny and G. Huysmans. Bezier surfaces and finite elements for MHD simulations. *Journal of Computational Physics*, 227, 7423 (2008).

M. Hölzl, S. Günter, R. P. Wenninger, et al. Reduced-magnetohydrodynamic simulations of toroidally and poloidally localized edge localized modes. *Physics of Plasmas*, 19, 082505 (2012a).

M. Hölzl, P. Merkel, G. Huysmans, et al. Coupling JOREK and STARWALL codes for non-linear resistive-wall simulations. *Journal of Physics: Conference Series*, 401, 012010 (2012b). doi:10.1088/1742-6596/401/1/012010.

G. Huysmans and O. Czarny. MHD stability in X-point geometry: simulation of ELMs. *Nuclear Fusion*, 47, 659 (2007).

I. Krebs, M. Hölzl, K. Lackner, et al. to be published (2013).

P. Merkel and M. Sempf. Feedback stabilization of resistive wall modes in the presence of multiply-connected wall structures. In *Proceedings of the 21st IAEA Fusion Energy Conference*. Chengdu, China (2006). TH/P3-8.

E. Strumberger, P. Merkel, C. Tichmann, et al. Linear stability studies in the presence of 3D wall structures. In *Proceedings of the 38th EPS Conference on Plasma Physics*. Strasbourg, France (2011). P5.082.

R. Wenninger, H. Zohm, J. Boom, et al. Solitary magnetic perturbations at the ELM onset. *Nuclear Fusion*, 42, 114025 (2012).

see also: www.ipp.mpg.de/∼mhoelzl

Acknowledgements

P. Merkel

I. Krebs

G. Huysmans

E. Nardon

S. Günter

K. Lackner

E. Strumberger

W.-C. Müller

Typical code run

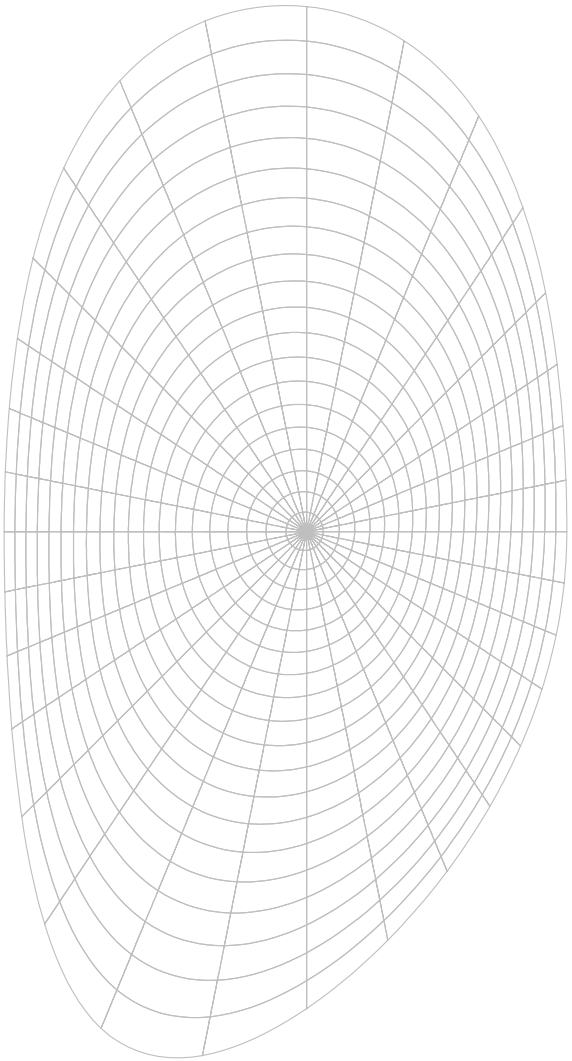

- Initial grid (Grids shown with reduced resolution)
- Equilibrium data (F_0, Ψ_{bnd}, profiles for T, ρ, FF')
- Grad-Shafranov
- Flux aligned grid (may include X-points)
- Radial and poloidal grid meshing
- Grad-Shafranov
- Axisymmetric flows
- Time-integration
- Analysis of restart-files:
  - Poincare plots
  - 2D or 3D VTK files
  - ...

Typical code run

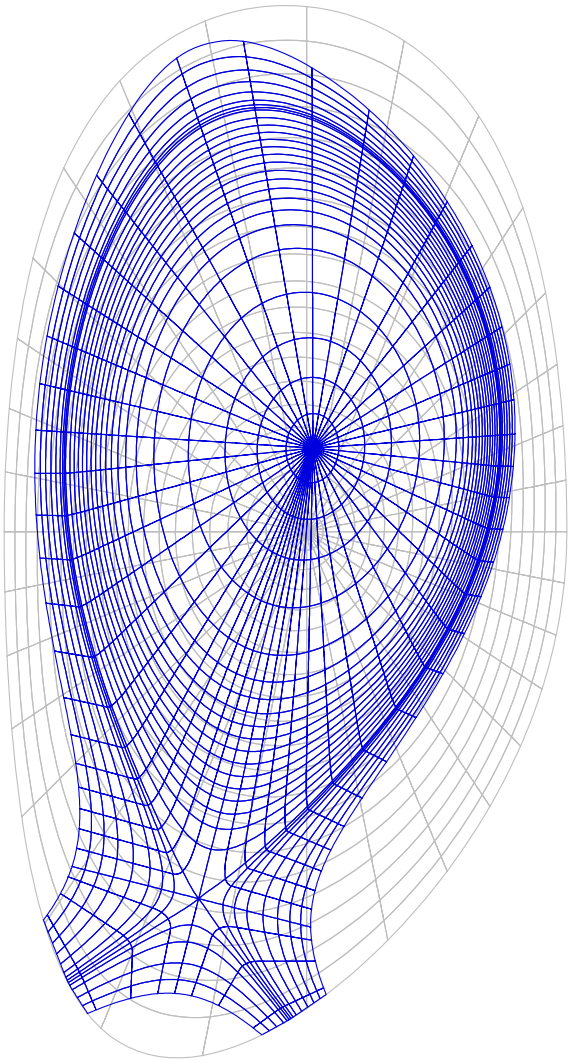

- Initial grid (Grids shown with reduced resolution)
- Equilibrium data (F_0, Ψ_{bnd}, profiles for T, ρ, FF')
- Grad-Shafranov
- Flux aligned grid (may include X-points)
- Radial and poloidal grid meshing
- Grad-Shafranov
- Axisymmetric flows
- Time-integration
- Analysis of restart-files:
  - Poincare plots
  - 2D or 3D VTK files
  - ...

Typical code run

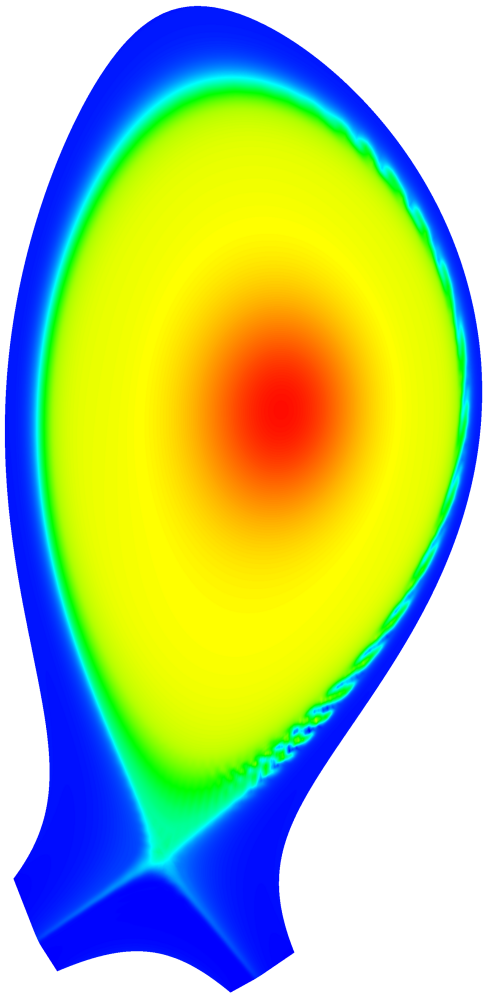

- Initial grid (Grids shown with reduced resolution)
- Equilibrium data (F_0, Ψ_{bnd}, profiles for T, ρ, FF')
- Grad-Shafranov
- Flux aligned grid (may include X-points)
- Radial and poloidal grid meshing
- Grad-Shafranov
- Axisymmetric flows
- Time-integration
- Analysis of restart-files:
  - Poincare plots
  - 2D or 3D VTK files
  - ...

Flux-algined X-point Grid

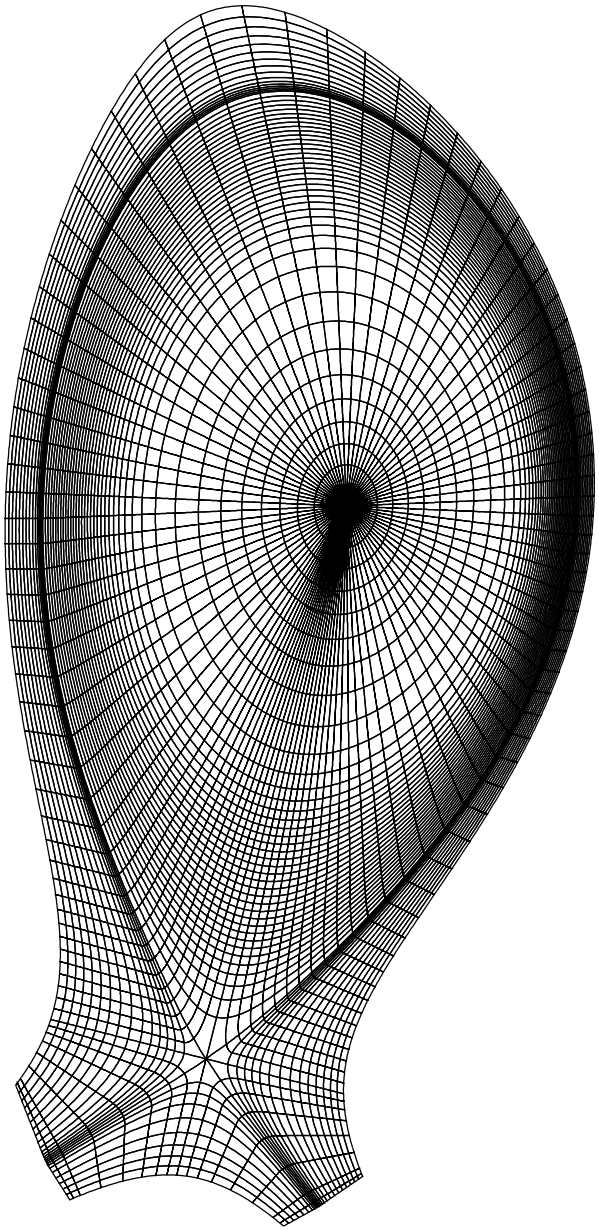

$$\frac{\partial p}{\partial t} = -\mathbf{v} \cdot \nabla p - \gamma p \nabla \cdot \mathbf{v} + \text{Diffusion} + \text{Source}$$

$$\frac{\partial (\rho T)}{\partial t} = -\mathbf{v} \cdot \nabla (\rho T) - \gamma \rho T \nabla \cdot \mathbf{v} + \nabla \cdot \left(K_{\perp} \nabla_{\perp} T + K_{||} \nabla_{||} T \right) + S_T$$

Input Profiles

- Input profiles taken from typical ASDEX Upgrade discharge:

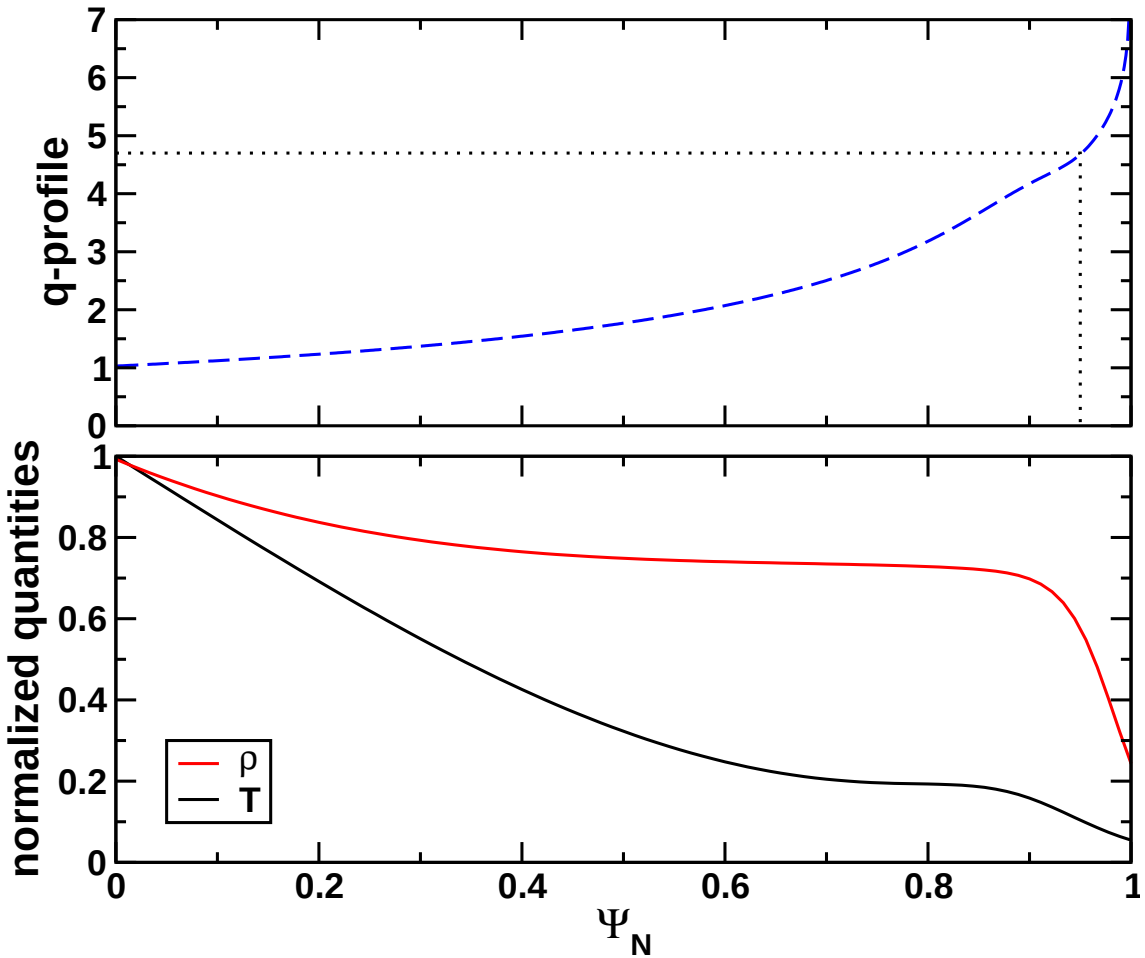

Ballooning Structure

- Mode-coupling causes localization of ballooning-filaments:

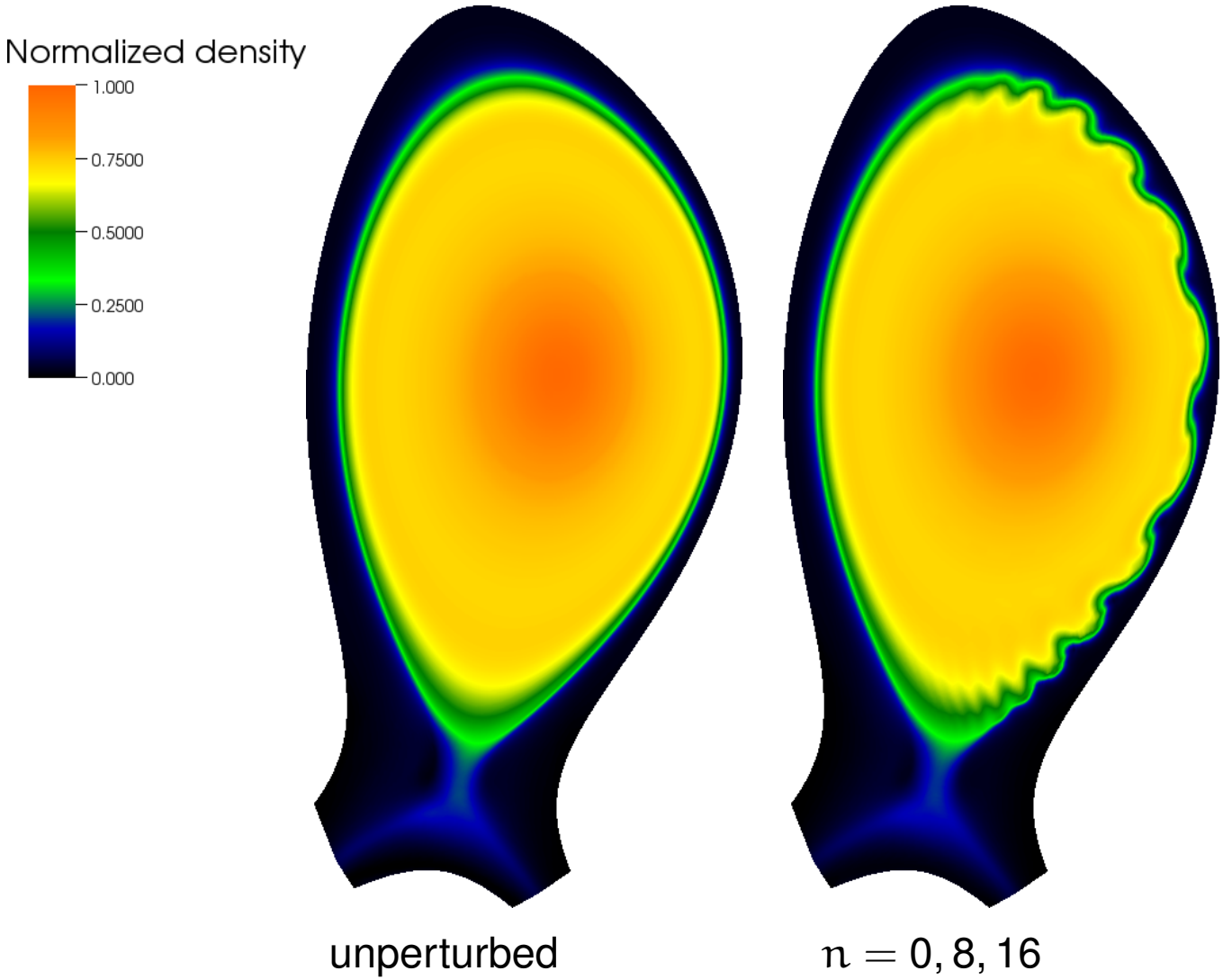

Ballooning Structure

- Mode-coupling causes localization of ballooning-filaments:

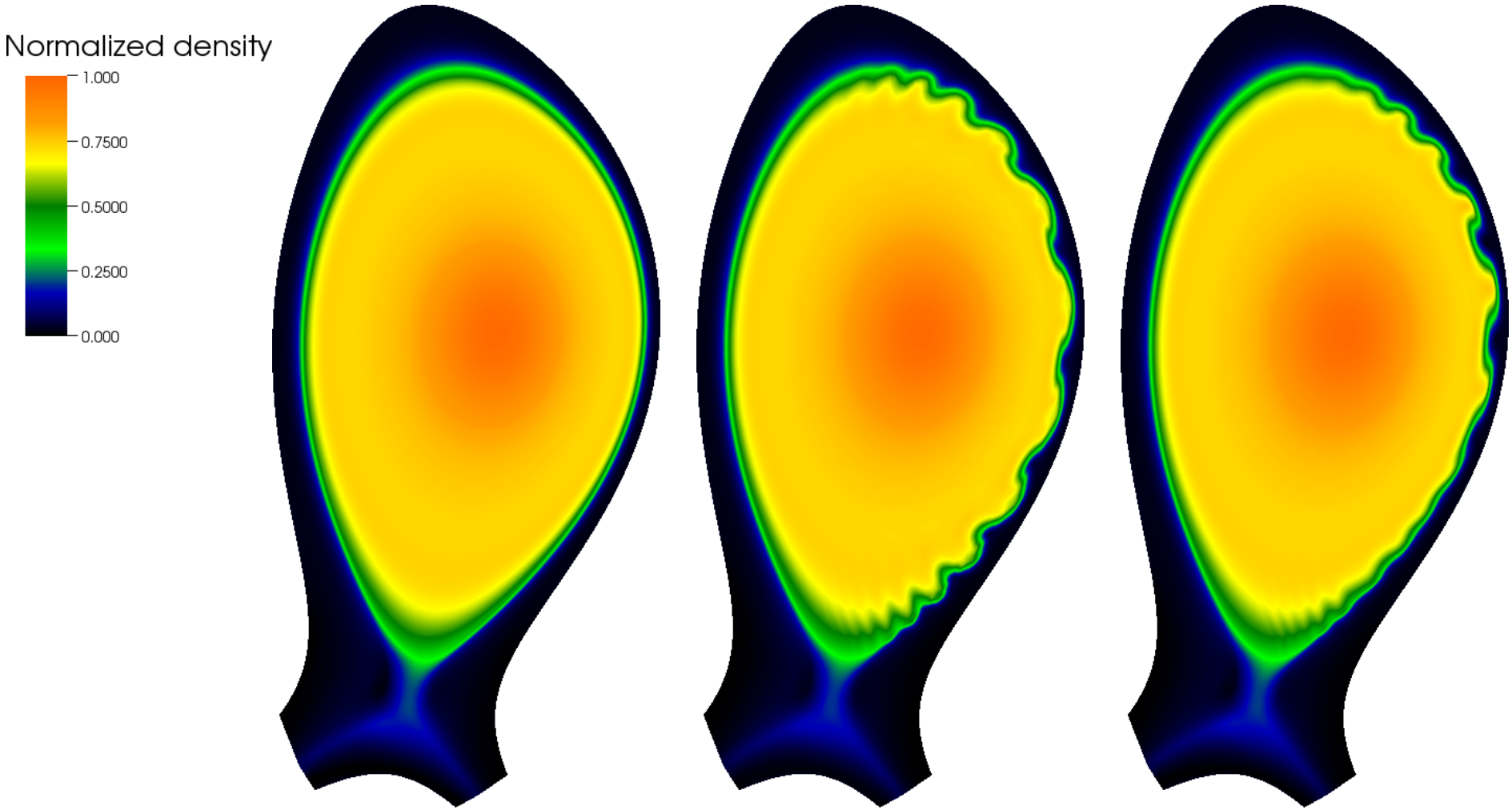

Position of Perturbations

- Radial perturbation positions differ between variables

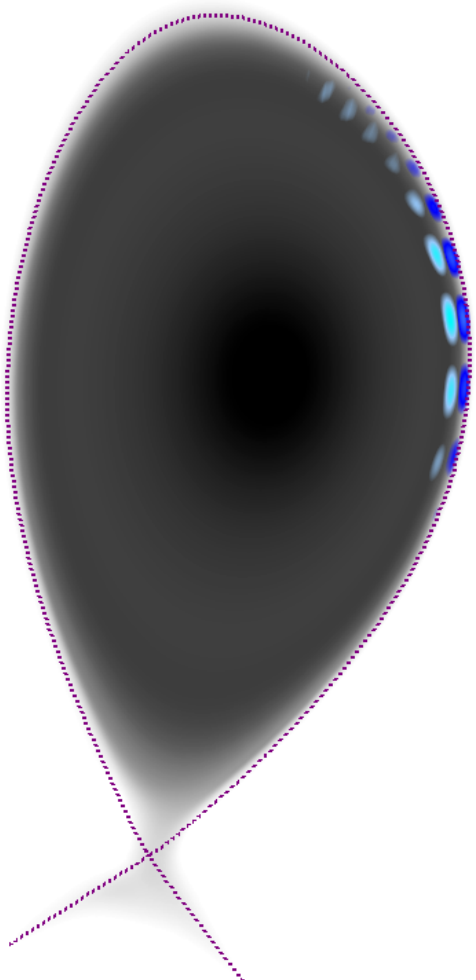

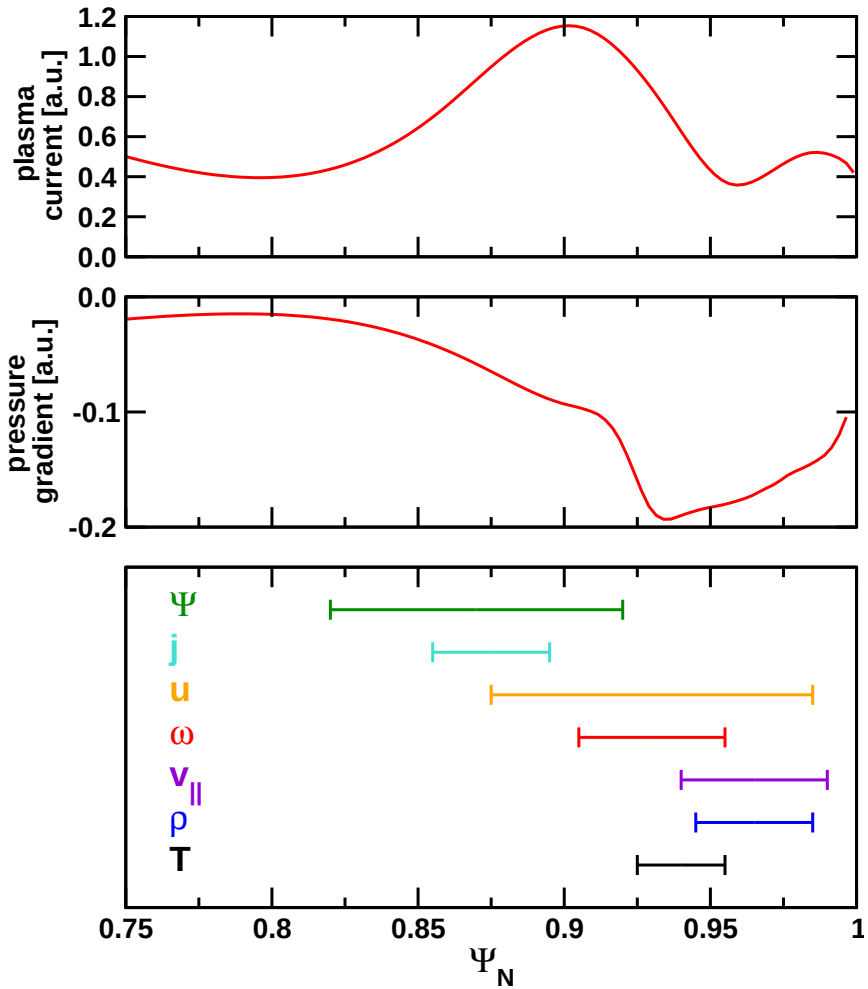

Influence of Wall

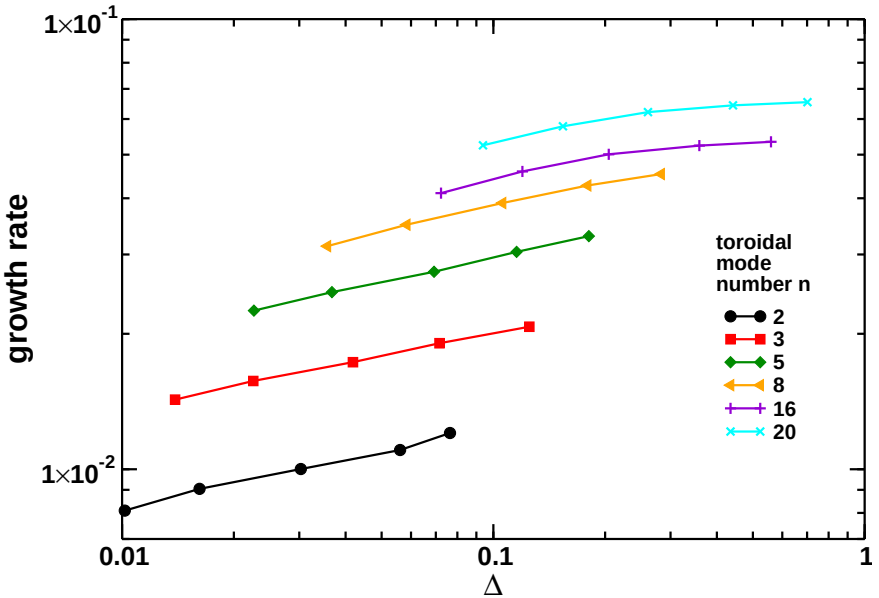

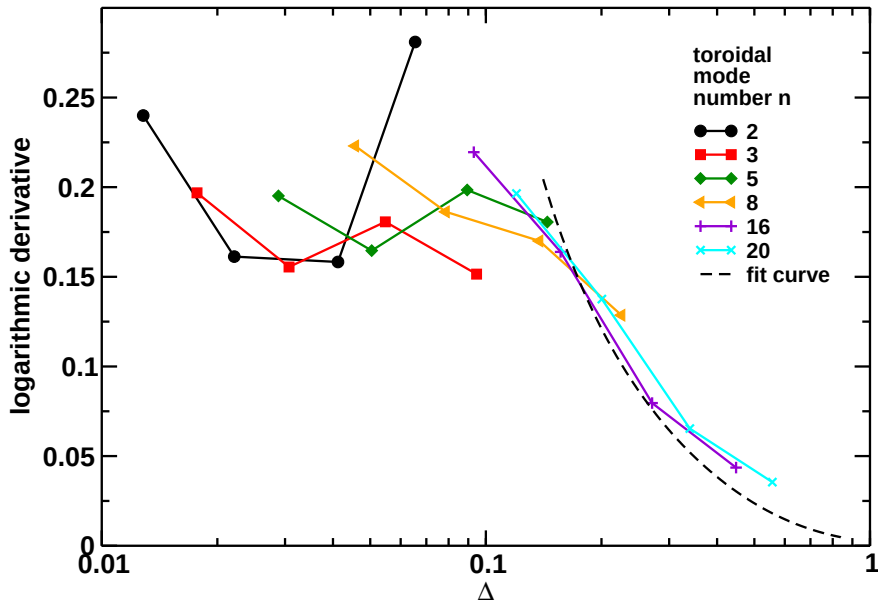

- Linear growth rate influenced by ideal wall boundary condition
- $\Delta =$ wall distance / poloidal mode half-width
- Wall effects become negligible if $\Delta \gtrsim 0.4$

Time Discretization

- Discretize consistently with other JOREK equations ($Y_k^{n+1} = Y_k^n + \delta Y_k^n$):

$$(1+\xi)\left[\delta Y_k^n + \sum_j \hat{M}_{k,j}^{ye}\ \delta\Psi_j^n\right] + \Delta t\ \theta\ \frac{\eta_w}{d_w}\ \hat{M}_{k,k}^{yy}\ \delta Y_k^n$$

$$= -\Delta t\ \frac{\eta_w}{d_w}\ \hat{M}_{k,k}^{yy}\ Y_k^n + \xi\left[\delta Y_k^{n-1} + \sum_j \hat{M}_{k,j}^{ye}\ \delta\Psi_j^{n-1}\right]$$

- Crank-Nicholson: ($\theta = 0.5$, $\xi = 0$) or Gears: ($\theta = 1$, $\xi = 0.5$)
- Solve for δY_k^n and insert into B_{tan} at time-step $n+1$:

$$B_{tan}^{n+1} = \sum_i b_i \left[\sum_j \hat{M}_{i,j}^{ee} \cdot \left(\Psi_j^n + \delta\Psi_j^n\right) + \sum_k \hat{M}_{i,k}^{ey} \cdot \left(Y_k^n + \delta Y_k^n\right)\right]$$

- Plug result into boundary integral $\oint dA\ \frac{j_i^*}{R}\ \underbrace{(\nabla\Psi \cdot \hat{\mathbf{n}}/R)}_{\equiv B_{tan}}$

Get this correct in Bezier formulation...

$$\sum_{i_{elem}} \int \frac{dV}{R^2} \left(j_i^* \, \delta j^n + \nabla j_i^* \cdot \nabla \delta \Psi^n \right) - \sum_{i_{bnd}} \oint dA \frac{j_i^*}{R} \sum_i b_i \sum_j \hat{E}_{i,j} \, \delta \Psi_j^n$$

$$= - \sum_{i_{elem}} \int \frac{dV}{R^2} \left(j_i^* \, j^n + \nabla j_i^* \cdot \nabla \Psi^n \right)$$

$$+ \sum_{i_{bnd}} \oint dA \frac{j_i^*}{R} \sum_i b_i \left[\sum_k \left(\hat{F}_{i,k} \, Y_k^n + \hat{G}_{i,k} \, \delta Y_k^{n-1} \right) + \sum_j \left(\hat{H}_{i,j} \, \Psi_j^n + \hat{J}_{i,j} \, \delta \Psi_j^{n-1} \right) \right]$$

and

$$Y_k^{n+1} = Y_k^n + \sum_j \hat{A}_{k,j} \, \delta \Psi_j^n + \hat{B}_{k,k} \, Y_k^n + \hat{C}_{k,k} \, \delta Y_k^{n-1} + \sum_j \hat{D}_{k,j} \, \delta \Psi_j^{n-1}$$

where

$$\hat{S}_{k,k} = 1 + \xi + \Delta t \theta \frac{\eta_w}{d_w} \hat{M}_{k,k}^{yy}$$
$$\hat{A}_{k,j} = -(1+\xi) \, \hat{M}_{k,j}^{ye} / \hat{S}_{k,k}$$
$$\hat{B}_{k,k} = -\Delta t \frac{\eta_w}{d_w} \hat{M}_{k,k}^{yy} / \hat{S}_{k,k}$$
$$\hat{C}_{k,k} = \xi / \hat{S}_{k,k}$$

$$\hat{D}_{k,j} = \xi \hat{M}_{k,j}^{ye} / \hat{S}_{k,k}$$
$$\hat{E}_{i,j} = \hat{M}_{i,j}^{ee} + \textstyle\sum_k \hat{M}_{i,k}^{ey} \, \hat{A}_{k,j}$$
$$\hat{F}_{i,k} = \hat{M}_{i,k}^{ey} (1 + \hat{B}_{k,k})$$
$$\hat{G}_{i,k} = \hat{M}_{i,k}^{ey} \, \hat{C}_{k,k}$$

$$\hat{H}_{i,j} = \hat{M}_{i,j}^{ee}$$
$$\hat{J}_{i,j} = \textstyle\sum_k \hat{M}_{i,k}^{ey} \, \hat{D}_{k,j}$$

and

$$\int dV = \sum_{i_{elem}} \int ds \, dt \, d\phi \, J_2 \, R$$

$$\oint dA = \sum_{i_{bnd}} \int dt \, d\phi \, R \sqrt{\left(\frac{\partial R}{\partial t} \right)^2 + \left(\frac{\partial Z}{\partial t} \right)^2}$$

Time evolution: GMRES and preconditioning

Generalized Minimum Residual Method (GMRES)

- $\hat{\mathcal{M}}\,\mathbf{x} = \mathbf{b}$ solved iteratively with GMRES
- Requests the following operations via reverse communication ("black box"):
  - Matrix-vector product $\rightarrow$ BLAS with OpenMP parallelization
  - Dot-product between two vectors $\rightarrow$ BLAS
  - Left preconditioning (right currently not used)

Time evolution: GMRES and preconditioning

Generalized Minimum Residual Method (GMRES)

- $\hat{\mathcal{M}}\ \mathbf{x} = \mathbf{b}$ solved iteratively with GMRES
- Requests the following operations via reverse communication ("black box"):
  - Matrix-vector product $\rightarrow$ BLAS with OpenMP parallelization
  - Dot-product between two vectors $\rightarrow$ BLAS
  - Left preconditioning (right currently not used)

Left Preconditioning

- Need to solve $\hat{\mathrm{P}}\ \mathbf{f} = \mathbf{g}$
- $\hat{\mathrm{P}}$: Matrix $\hat{\mathcal{M}}$ without coupling terms between toroidal harmonics

$\Rightarrow$ Block-diagonal matrix with few large sparse blocks

- Solve decoupled block-systems with direct solver PaStiX